Editors' Suggestion Featured in Physics

# Evidence of Large Recoil Velocity from a Black Hole Merger Signal

Vijay Varma,[1,*] Sylvia Biscoveanu,[2,3] Tousif Islam,[4,5] Feroz H. Shaik,[4,5] Carl-Johan Haster,[2,3] Maximiliano Isi,[6] Will M. Farr,[7,6] Scott E. Field,[4,5] and Salvatore Vitale[2,3]

[1]*Max Planck Institute for Gravitational Physics (Albert Einstein Institute), Am Mühlenberg 1, Potsdam 14476, Germany*

[2]*LIGO Laboratory, Massachusetts Institute of Technology, Cambridge, Massachusetts 02139, USA*

[3]*Department of Physics and Kavli Institute for Astrophysics and Space Research, Massachusetts Institute of Technology, 77 Massachusetts Ave, Cambridge, Massachusetts 02139, USA*

[4]*Department of Mathematics, University of Massachusetts, Dartmouth, Massachusetts 02747, USA*

[5]*Center for Scientific Computing and Data Science Research, University of Massachusetts, Dartmouth, Massachusetts 02747, USA*

[6]*Center for Computational Astrophysics, Flatiron Institute, New York, New York 10010, USA*

[7]*Department of Physics and Astronomy, Stony Brook University, Stony Brook, New York 11794, USA*

(Received 11 January 2022; revised 10 March 2022; accepted 11 April 2022; published 12 May 2022)

The final black hole left behind after a binary black hole merger can attain a recoil velocity, or a "kick," reaching values up to 5000 km/s. This phenomenon has important implications for gravitational wave astronomy, black hole formation scenarios, testing general relativity, and galaxy evolution. We consider the gravitational wave signal from the binary black hole merger GW200129_065458 (henceforth referred to as GW200129), which has been shown to exhibit strong evidence of orbital precession. Using numerical relativity surrogate models, we constrain the kick velocity of GW200129 to $v_f \sim 1542^{+747}_{-1098}$ km/s or $v_f \gtrsim 698$ km/s (one-sided limit), at 90% credibility. This marks the first identification of a large kick velocity for an individual gravitational wave event. Given the kick velocity of GW200129, we estimate that there is a less than 0.48% (7.7%) probability that the remnant black hole after the merger would be retained by globular (nuclear star) clusters. Finally, we show that kick effects are not expected to cause biases in ringdown tests of general relativity for this event, although this may change in the future with improved detectors.

DOI: 10.1103/PhysRevLett.128.191102

*Introduction.*—When two black holes (BHs) orbit each other, they emit gravitational waves (GWs) which carry away energy and angular momentum. This causes the orbit to shrink in a runaway process that culminates in the merger of the BHs into a single remnant BH. At the same time, the GWs can also carry away linear momentum from the binary, shifting its center of mass in the opposite direction [1]. Most of the linear momentum is lost near the merger [2], resulting in a recoil or "kick" velocity imparted to the remnant BH.

Kicks are particularly striking for precessing binaries, in which the component BH spins are tilted with respect to the orbital angular momentum. For these systems, the spins interact with the orbital angular momentum as well as with each other, causing the orbital plane to precess [3]. Numerical relativity (NR) simulations revealed that the kick velocities for precessing binaries can reach values up to ~5000 km/s [4–6], large enough to be ejected from any host galaxy [7].

Kicks have important implications for BH astrophysics. Following a supermassive BH merger, the remnant BH can be displaced from the galactic center or ejected entirely [7], impacting the galaxy's evolution [8], fraction of galaxies with central supermassive BHs [9], and event rates [10] for the future LISA mission [11]. For stellar-mass BHs like those observed by LIGO [12] and Virgo [13], kicks can limit the formation of heavy BHs. BH masses greater than ~65 $M_\odot$ are disfavored by supernova simulations [14,15], but have been seen in GW events [16–18]. This could be explained by second-generation mergers [19], in which one of the component BHs is itself a remnant from a previous merger, and is thus more massive than the original stellar-mass progenitors. However, if the kick from the first merger is large enough, the remnant BH would get ejected from its host galaxy and would not participate in another merger.

Unfortunately, observational evidence of large kicks has been elusive. While various candidates from electromagnetic observations have been identified, their nature is debated [20]. Similarly, observing kicks using GW signals has been challenging [21–27]. For example, Varma *et al.* [21] used accurate models based on NR simulations to show that kicks from precessing binaries can be reliably inferred with LIGO-Virgo operating at their design sensitivity. However, the GW events analyzed in Ref. [21], which only included signals in the first two LIGO-Virgo observing runs [28], were not loud enough to constrain the kick.

Since then, the LIGO-Virgo detectors have been further upgraded, and the GW data from the third observing run were released in two stages, *O*3*a* [17] and *O*3*b* [18]. Notably, *O*3*a* provided the first evidence for precession in the ensemble population of merging binaries [29], even though none of the individual GW events unambiguously exhibited precession [17]. Finally, in *O*3*b*, the binary BH merger GW200129 was identified as the first individual GW event showing strong evidence of precession [18,30]. Similarly, support for large kicks was identified in the ensemble population using the *O*3*a* data [31,32], even though the individual events were not loud enough for an unambiguous kick inference [21,33] (with the exception of GW190814 [34], which was found to have a *small* kick of $\sim 74^{+10}_{-7}$ km/s at 90% credibility [27]).

In this Letter, we use the method developed in Ref. [21] to show that GW200129 has a large kick velocity ($\sim 1542^{+747}_{-1098}$ km/s at 90% credibility). As an application of the kick constraint, we compute the retention probability for the remnant BH of GW200129 in various host environments, and discuss the implications for the formation of heavy stellar-mass BHs. Finally, we show that Doppler effects due to the kick on the remnant mass measurement are small for this event, and should not impact ringdown tests of general relativity (GR).

*Methods.*—We follow the procedure outlined in Ref. [21] to infer the kick from a GW signal. We begin by measuring the binary source parameters following Bayes' theorem [35]:

$$p(\boldsymbol{\lambda}|d) \propto \mathcal{L}(d|\boldsymbol{\lambda})\pi(\boldsymbol{\lambda}), \tag{1}$$

where $p(\boldsymbol{\lambda}|d)$ is the *posterior* probability distribution of the binary parameters $\boldsymbol{\lambda}$ given the observed data $d$, $\mathcal{L}(d|\boldsymbol{\lambda})$ is the *likelihood* of the data given $\boldsymbol{\lambda}$, and $\pi(\boldsymbol{\lambda})$ is the *prior* probability distribution for $\boldsymbol{\lambda}$. Under the assumption of Gaussian detector noise, the likelihood $\mathcal{L}(d|\boldsymbol{\lambda})$ can be evaluated for any $\boldsymbol{\lambda}$ using a gravitational waveform model and the observed data stream $d$ [35]. A stochastic sampling algorithm is then used to draw *posterior samples* for $\boldsymbol{\lambda}$ from $p(\boldsymbol{\lambda}|d)$. We use the `Parallel Bilby` [36] parameter estimation package with the `dynesty` [37] sampler.

For quasicircular binary BHs, the full set of parameters $\boldsymbol{\lambda}$ is 15 dimensional [18]. This includes the 8D intrinsic parameters: the component masses ($m_1$ and $m_2$) and spins ($\boldsymbol{\chi}_1$ and $\boldsymbol{\chi}_2$, each of which is a 3D vector), as well as the 7D extrinsic parameters: the distance, right ascension, declination, time of arrival, coalescence phase, binary inclination, and polarization angle. Here, index 1 (2) corresponds to the heavier (lighter) BH, $\boldsymbol{\chi}_{1,2}$ are dimensionless spins with magnitudes $\chi_{1,2} \leq 1$, and masses refer to the detector frame redshifted masses. We also define the mass ratio $q = m_1/m_2 \geq 1$, total mass $M = m_1 + m_2$, and use geometric units with $G = c = 1$.

We employ the NR surrogate models `NRSur7dq4` [38] and `NRSur7dq4Remnant` [38,39] to infer the kick. Constructed by effectively interpolating between $\sim 1500$ precessing NR simulations, `NRSur7dq4` predicts the gravitational waveform, while `NRSur7dq4Remnant` predicts the mass $m_f$, spin $\boldsymbol{\chi}_f$, and kick velocity $\boldsymbol{v}_f$ of the remnant BH. We first obtain posterior samples for all 15 binary parameters using `NRSur7dq4`. The spins are measured in a source frame defined at a given reference point (see below): the $z$ axis lies along the instantaneous orbital angular momentum, the $x$ axis points along the line of separation from the lighter to the heavier BH, and the $y$ axis completes the right-handed triad. The remnant properties, which are also defined in the same source frame, depend only on the intrinsic parameters $\boldsymbol{\Lambda} = \{m_1, m_2, \boldsymbol{\chi}_1, \boldsymbol{\chi}_2\}$. Therefore, the posteriors for the remnant properties are obtained by evaluating `NRSur7dq4Remnant` on the $\boldsymbol{\Lambda}$ posterior samples; put simply, `NRSur7dq4Remnant` is a function of $\boldsymbol{\Lambda}$ that yields $m_f$, $\boldsymbol{\chi}_f$, and $\boldsymbol{v}_f$. We also compute the *effective prior* distribution for $\boldsymbol{v}_f$, by evaluating `NRSur7dq4Remnant` on $\boldsymbol{\Lambda}$ samples drawn from the prior $\pi(\boldsymbol{\Lambda})$. The difference between the kick posterior and prior can be used to gauge how informative the data are about the kick [21].

Traditional modeling methods assume a phenomenological ansatz for the waveform [40,41] or remnant properties [42–45], and calibrate remaining free parameters to NR simulations. NR surrogate methods [38,39,46,47], on the other hand, take a data-driven approach, and the models are trained directly against precessing NR simulations. In this approach, one first constructs a suitable numerical basis using a subset of the NR waveforms, and then builds fits across parameter space for the basis coefficients; we refer the reader to Ref. [38] for more details. NR surrogate models do not need to introduce additional assumptions about the underlying phenomenology which would necessarily introduce some systematic error. Through cross-validation studies, it has been shown that both `NRSur7dq4` and `NRSur7dq4Remnant` achieve accuracies comparable to the simulations themselves [38], and as a result, are the most accurate models currently available for precessing systems, within their parameter space of validity: both models are trained on simulations with $q \leq 4$ and $\chi_{1,2} \leq 0.8$, but can be extrapolated to $q \leq 6$ and $\chi_{1,2} \leq 1$ [38]. As GW200129 shows significant support for large spins, we conduct some tests of the surrogate models in this regime in the Supplemental Material [48].

For the prior in Eq. (1), we follow Ref. [18] and adopt a uniform prior for spin magnitudes (with $0 \leq \chi_1, \chi_2 \leq 0.99$) and redshifted component masses; an isotropic prior for spin orientations, sky location, and binary orientation; and a distance prior (`UniformSourceFrame` [55]) that assumes uniform source distribution in comoving volume and time. In addition, we place the following constraints: $q \leq 6$ and $60 \leq M \leq 400$. These constraints are motivated by the regime of validity of `NRSur7dq4` [38], and are broad enough to safely encompass the posterior spread of GW200129 [18].

Because the spin directions are not constant for precessing binaries, spin measurements are inherently tied to a specific moment in the binary's evolution. The standard approach is to measure the spins at the point where the frequency of the GW signal at the detector reaches a prespecified reference value, typically $f_{\mathrm{ref}} = 20$ Hz [17]. This is mainly motivated by the fact that the sensitivity band of current detectors begins near this value [12,13]. However, Ref. [56] recently showed that constraints on orbital-plane spin directions can be greatly improved by measuring the spins near the merger, in particular, at a fixed *dimensionless* reference time $t_{\mathrm{ref}}/M = -100$ before the peak of the GW amplitude. This improvement can be attributed to the waveform being more sensitive to variations in the orbital-plane spin directions near the merger [56] ($t_{\mathrm{ref}}/M = -100$ typically falls within ∼2–4 GW cycles before the peak amplitude, independent of the binary parameters [56].).

We will adopt the $t_{\mathrm{ref}}/M = -100$ reference point for the main results in this Letter, but will show a comparison against $f_{\mathrm{ref}} = 20$ Hz for completeness. As we will discuss below, the choice of reference point has a negligible impact on the kick inference itself, but comparing the spin posteriors at the two reference points helps illustrate why a kick constraint is possible in the first place. As a bonus, spin measurements at $t_{\mathrm{ref}}/M = -100$ are convenient for inferring the kick as the `NRSur7dq4Remnant` model is also trained at this reference time [38]; this choice was found to lead to a more accurate remnant BH model in Refs. [38,39].

*GW200129 spin measurements.*—GW200129 is the first GW event showing strong signs of precession [18,30]. Figure 1 shows the posterior distribution for the mass ratio and spin parameters obtained using the `NRSur7dq4` model at reference points $t_{\mathrm{ref}}/M = -100$ and $f_{\mathrm{ref}} = 20$ Hz; our constraints at $f_{\mathrm{ref}} = 20$ Hz are consistent with those of Ref. [30]. The spin vectors $\boldsymbol{\chi}_{1,2}$ are decomposed into magnitudes $\chi_{1,2}$, tilt angles $\theta_{1,2}$ with respect to the

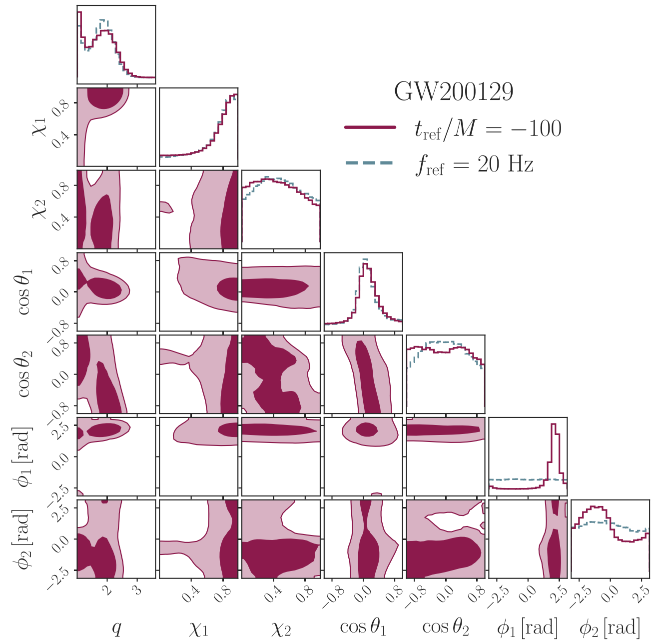


FIG. 1. Constraints on the mass ratio and spins for GW200129, at reference time $t_{\mathrm{ref}}/M = -100$. The dark (light) regions represent the 50% (90%) credible bounds on joint 2D posteriors, while the diagonal plots show 1D marginalized posteriors. There is a preference for large $\chi_1$ and $\cos\theta_1 \sim 0$, meaning there is substantial spin in the orbital plane, which leads to precession. For comparison, we also show the 1D marginalized posteriors at $f_{\mathrm{ref}} = 20$ Hz. The azimuthal spin angles (especially $\phi_1$) are much better constrained at $t_{\mathrm{ref}}/M = -100$; this is critical for constraining the kick.

$z$ axis, and azimuthal angles $\phi_{1,2}$ with respect to the $x$ axis of the source frame. Because of precession, spin measurements vary between the two reference points but can be related by a spin evolution [38,56].

For both reference points in Fig. 1, there is a clear preference for large orbital-plane spins for the heavier BH (large $\chi_1$ and $\cos\theta_1 \sim 0$). Even though the spin of the lighter BH is not well measured, this is sufficient for precession. We stress that while precessing binaries tend to have larger kicks [4–6], precession does not necessarily imply a large kick, and it is important to directly compute the kick velocity as we do in the next section. In particular, the kick can vary from zero to ∼5000 km/s just by changing the azimuthal spin angles, even for systems with large orbital-plane spins [4–6].

Next, the azimuthal angles (especially $\phi_1$) in Fig. 1 are much better constrained at $t_{\mathrm{ref}}/M = -100$, while the other parameters do not change significantly [57]. This feature is key: even though the azimuthal angles are poorly constrained in the inspiral, they are well constrained at $t_{\mathrm{ref}}/M = -100$ [56]. As the kick depends sensitively on the azimuthal angles near the merger [4], successfully measuring these angles at $t_{\mathrm{ref}}/M = -100$ is critical for constraining the kick.

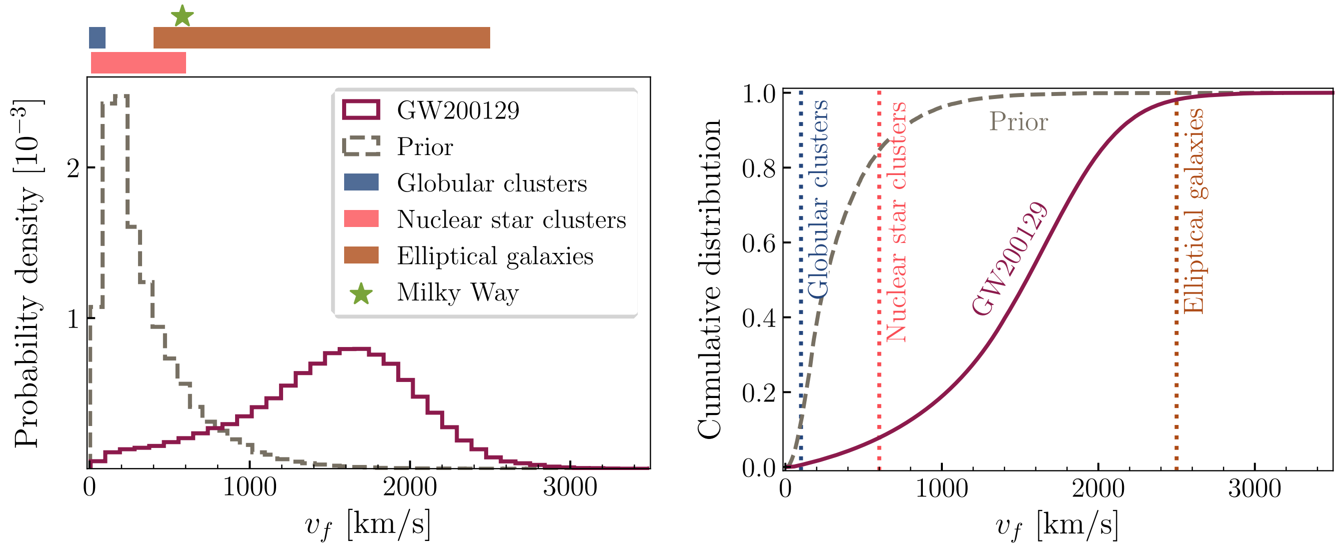


FIG. 2. Left: kick magnitude constraints for GW200129. We show the posterior and the effective prior, along with known ranges for the escape velocities for various types of host environments for comparison. There is a clear preference for large kicks in the posterior, with $v_f \gtrsim 698$ km/s at 90% credibility. Right: CDFs for the kick posterior and prior. The upper bounds of the escape velocity ranges from the left panel are shown as vertical dotted lines. The upper limit for retention probability of the merger remnant is given by the intersection of these lines with the posterior CDF.

Spins measured at $f_{\mathrm{ref}} = 20$ Hz can also be evolved consistently to $t_{\mathrm{ref}}/M = -100$ using NRSur7dq4 dynamics [38]. In fact, this procedure is internally applied by NRSur7dq4Remnant if the spins are specified at $f_{\mathrm{ref}} = 20$ Hz [38,39]. Therefore, by construction, the kick posterior for individual GW events is independent of the reference point at which the spins are initially measured (modulo NRSur7dq4 spin evolution errors, which are small compared with the model errors [38,47]). Therefore, for the purpose of this Letter, the main benefit of the spin measurements at $t_{\mathrm{ref}}/M = -100$ is to illustrate why a successful kick constraint is possible in the first place. The supplement of Ref. [31] discusses other benefits, in particular, for constraining the ensemble population of spins and kicks. In the rest of the Letter, we will use the spin measurements at $t_{\mathrm{ref}}/M = -100$.

As noted in Refs. [18,30], the inference of precession in GW200129 depends on the waveform model used. In particular, while the phenomenological model IMRPhenomXPHM [40] recovers precession, the effective-one-body model SEOBNRv4PHM [41] does not. Among these models, only NRSur7dq4 is informed by precessing NR simulations and is more accurate by about one order of magnitude [38]. By contrast, SEOBNRv4PHM and IMRPhenomXPHM approximate precession effects by "twisting" the frame of an equivalent aligned-spin binary [40,41]. Furthermore, Ref. [56] found that NRSur7dq4 is necessary to accurately measure the spin vectors $\chi_{1,2}$, in particular, the spin directions within the orbital plane [56], which have a strong influence on the kick [4]. Similarly, given the spin measurements, NRSur7dq4Remnant is necessary to accurately predict the kick velocity [21]. For these reasons, we treat NRSur7dq4 and NRSur7dq4Remnant as the preferred models for analyzing GW200129.

*GW200129 kick velocity.*—Figure 2 shows our constraints on the kick magnitude $v_f$ of GW200129, obtained by evaluating NRSur7dq4Remnant on the NRSur7dq4 $\mathbf{\Lambda}$ posteriors at $t_{\mathrm{ref}}/M = -100$. In the left panel, we show the posterior and prior distributions for $v_f$, along with fiducial escape velocities for globular clusters [58], nuclear star clusters [58], giant elliptical galaxies [7], and Milky Way-like galaxies [59] for comparison. Unlike the events considered in Ref. [21], the $v_f$ posterior is clearly distinguishable from the prior, and there is substantial information gain about the kick [60].

The kick magnitude is constrained to $v_f \sim 1542^{+747}_{-1098}$ km/s (median and 90% symmetric credible interval), or $v_f \gtrsim 698$ km/s (lower tenth percentile), making GW200129 the first GW event identified as having a large kick velocity. We note, however, that such large kick velocities are not surprising given previous constraints on the ensemble properties of merging binary BHs [31,32]. For example, Fig. 3 of Ref. [31], which shows estimates of the ensemble kick distribution, includes non-neglibile support up to $v_f \sim 1500$ km/s.

The large kick of GW200129 raises the question of whether the remnant BH is ejected from its host environment. This has implications for the formation of heavy BHs through second-generation mergers in dense environments [19]. This formation channel is one possible way to explain observations of BHs with masses $\gtrsim 65\ M_\odot$ [16–18], which fall within the mass gap expected due to the (pulsational) pair-instability supernova processes [14,15]. To address this, we compute the retention probability for the remnant BH of GW200129 in globular clusters and nuclear star clusters, both of which host dense stellar environments where merger remnants can potentially interact with other BHs and form binaries.

The right panel of Fig. 2 shows the cumulative distribution functions (CDFs) for the $v_f$ posterior and prior. As the posterior CDF($v_f$) denotes the probability that the kick magnitude of GW200129 is below $v_f$, we take it to be the probability that the remnant BH is retained by a host environment with an escape velocity of $v_f$. The vertical dotted lines indicate the maximum escape velocity $v_{\rm esc}^{\rm max}$ for various host environments; CDF($v_{\rm esc}^{\rm max}$) sets the upper limit on the retention probability for that host. In particular, assuming $v_{\rm esc}^{\rm max} = 100$ km/s ($v_{\rm esc}^{\rm max} = 600$) for globular (nuclear star) clusters there is a less than 0.48% (7.7%) probability that the remnant BH of GW200129 is retained by those hosts. This is consistent with Refs. [31,32], where globular clusters were already identified as an unlikely site for second-generation mergers, even for more moderate kicks.

*Remnant mass and Doppler shifts.*—Our method provides predictions for both the magnitude and direction of the kick [21]. If the kick vector $\boldsymbol{v}_f$ has a significant component along (or opposite) the line of sight, the observed GW signal can be influenced by the kick. At leading order, the kick's effect can be described as a Doppler shift of the GW frequency [23]. However, as GR lacks any intrinsic length scales, a uniform increase in signal frequency is completely degenerate with a decrease in total mass $M$, and vice versa. Thus, if not explicitly accounted for, a frequency shift due to a kick can bias mass measurements. In particular, because the kick is mostly imparted near the merger [2], the Doppler shift only affects the merger and ringdown part of the signal. This can lead to biases in the measurement of the remnant mass $m_f$ [21,62], and potentially impact tests of GR using the ringdown signal [63]. However, this effect is expected to be small for current detectors [21,23].

In the following, we verify that the Doppler effect on the remnant mass measurement of GW200129 is indeed small. At leading order, the Doppler-shifted remnant mass is given by [23]

$$m_f^{\rm DS} = m_f(1 + \boldsymbol{v}_f \cdot \hat{\boldsymbol{n}}/c), \qquad (2)$$

where $c$ is the speed of light and $\hat{\boldsymbol{n}}$ is the unit vector pointing along the line of sight from the observer to the source. The line of sight direction is obtained from our inference setup, parametrized by ($\iota$, $\phi$). $\iota$ is the inclination angle between the orbital angular momentum and the line of sight to the observer, and $\phi$ is the azimuthal angle to the observer in the orbital plane, both defined in the source frame at $t_{\rm ref}/M = -100$.

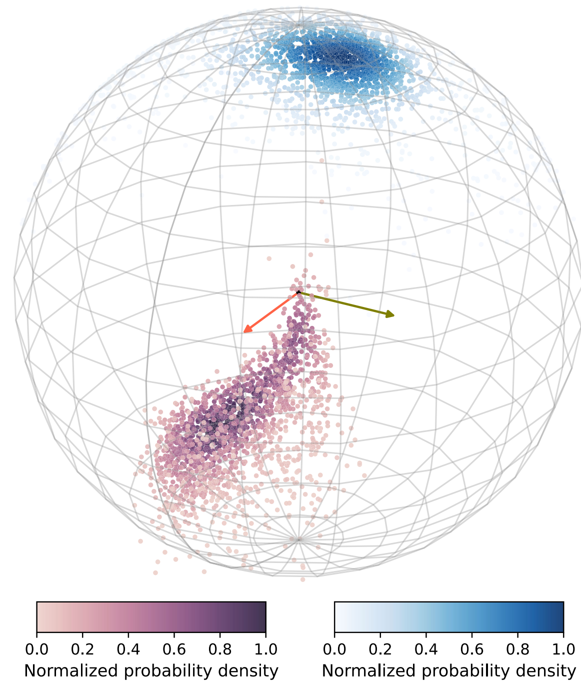


FIG. 3. Posterior samples for the full kick vector $\boldsymbol{v}_f$ in the source frame at $t_{\rm ref}/M = -100$. Each purple marker indicates a kick posterior sample; an arrow drawn from the origin to the marker would show the kick vector $\boldsymbol{v}_f$. The outer radius of the sphere corresponds to $v_f = 2500$ km/s. The $x$ axis (orange) and $y$ axis (green) are shown as arrows near the origin; the $x$-$y$ plane is orthogonal to the orbital angular momentum direction. The blue markers on the sphere show posterior samples for the line-of-sight direction to the observer. For both distributions, the spread represents the measurement uncertainty, and the color reflects posterior probability density (normalized so that the peak density is 1). A rotating perspective of this plot can be seen at Ref. [64].

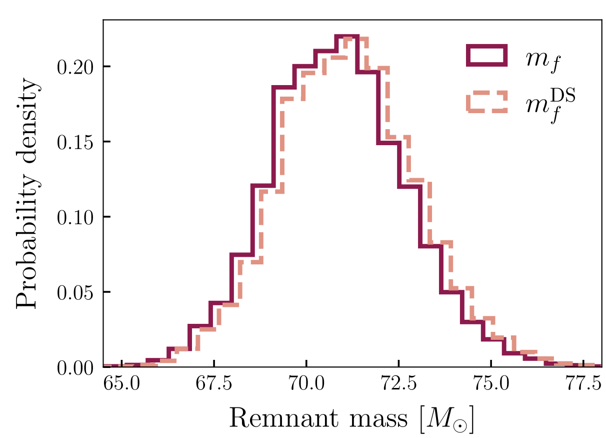


FIG. 4. The remnant mass and the Doppler shifted remnant mass for GW200129, as inferred in the detector frame. There is an overall redshift, as the kick direction in Fig. 3 is pointed (roughly) away from the observer. However, as these distributions are very close, we do not expect ringdown tests of GR to be impacted by the kick for this event.

Figure 3 shows the posterior distributions for the full kick vector $\boldsymbol{v}_f$ (also defined in the source frame at $t_{\mathrm{ref}}/M = -100$) and the line-of-sight direction. We find that the kick and the line-of-sight are not very well (anti-) aligned; therefore, we do not expect significant Doppler shifts for this signal. Finally, Fig. 4 shows the posterior distributions for $m_f$ (obtained from NRSur7dq4Remnant) and $m_f^{\mathrm{DS}}$ [computed using Eq. (2)] for GW200129. As expected, the difference between these distributions is very small compared with the measurement uncertainty, meaning that tests of GR should not be impacted by the Doppler effect for this event. As detector sensitivity improves, this may not be the case, however, and it may be necessary to explicitly account for this effect [21].

*Conclusions.*—We use NR surrogate models for the gravitational waveform and the remnant BH properties to infer the kick velocity for the binary BH merger GW200129. The kick magnitude is constrained to $v_f \sim 1542^{+747}_{-1098}$ km/s or $v_f \gtrsim 698$ km/s, at 90% credibility. Given the kick velocity, we estimate that there is at most a 0.48% (7.7%) probability that the remnant BH of GW200129 would be retained by globular (nuclear star) clusters. Finally, we show that the Doppler effect on the remnant mass is small compared with current measurement uncertainty; therefore ringdown tests of GR are not expected to be significantly impacted by the kick for this event.

Observational evidence for kicks has far reaching implications for BH astrophysics. GW200129 is the first GW event identified as having a large kick velocity. Large kicks like this have been previously predicted based on the ensemble kick distribution of merging binary BHs [31,32], and we can expect to see more such events as detector sensitivity improves. In particular, such observations can help resolve the mystery of the heavy BHs seen by LIGO-Virgo [16–18], by constraining the rate of second-generation mergers.

We thank Arif Shaikh for comments on the manuscript. V. V. acknowledges funding from the European Union's Horizon 2020 research and innovation program under the Marie Skłodowska-Curie Grant Agreement No. 896869. S. B., C.-J. H., and S. V. acknowledge support of the National Science Foundation (NSF) and the LIGO Laboratory. S. B. is also supported by the NSF Graduate Research Fellowship under Grant No. DGE-1122374. S. V. is also supported by NSF Grant No. PHY-2045740. T. I. is supported by the Heising-Simons Foundation, the Simons Foundation, and NSF Grants No. PHY-1748958, No. PHY-1806665, and No. DMS-1912716. F. S. and S. E. F. are supported by NSF Grants No. PHY-2110496 and No. PHY-1806665. Computations were performed on the Wheeler cluster at Caltech, which is supported by the Sherman Fairchild Foundation and by Caltech; and the High Performance Cluster at Caltech. This material is based upon work supported by NSF's LIGO Laboratory which is a major facility fully funded by the NSF. LIGO was constructed by the California Institute of Technology and Massachusetts Institute of Technology with funding from the NSF and operates under cooperative Agreement No. PHY-0757058. This research made use of data, software and/or web tools obtained from the Gravitational Wave Open Science Center [65], a service of the LIGO Laboratory, the LIGO Scientific Collaboration, and the Virgo Collaboration.

[*]vijay.varma@aei.mpg.de

[1] M. J. Fitchett, The influence of gravitational wave momentum losses on the centre of mass motion of a Newtonian binary system, Mon. Not. R. Astron. Soc. **203**, 1049 (1983).

[2] José A. Gonzalez, U. Sperhake, B. Brüegmann, M. Hannam, and S. Husa, Total Recoil: The Maximum Kick from Non-spinning Black-Hole Binary Inspiral, Phys. Rev. Lett. **98**, 091101 (2007).

[3] Theocharis A. Apostolatos, Curt Cutler, Gerald J. Sussman, and Kip S. Thorne, Spin-induced orbital precession and its modulation of the gravitational waveforms from merging binaries, Phys. Rev. D **49**, 6274 (1994).

[4] Manuela Campanelli, Carlos O. Lousto, Yosef Zlochower, and David Merritt, Maximum Gravitational Recoil, Phys. Rev. Lett. **98**, 231102 (2007).

[5] J. A. González, M. Hannam, U. Sperhake, Bernd Brüegmann, and S. Husa, Supermassive Recoil Velocities for Binary Black-Hole Mergers with Antialigned Spins, Phys. Rev. Lett. **98**, 231101 (2007).

[6] Carlos O. Lousto and Yosef Zlochower, Hangup Kicks: Still Larger Recoils by Partial Spin/Orbit Alignment of Black-Hole Binaries, Phys. Rev. Lett. **107**, 231102 (2011).

[7] David Merritt, Milos Milosavljevic, Marc Favata, Scott A. Hughes, and Daniel E. Holz, Consequences of gravitational radiation recoil, Astrophys. J. **607**, L9 (2004).

[8] S. Komossa and David Merritt, Gravitational wave recoil oscillations of black holes: Implications for unified models of active galactic nuclei, Astrophys. J. **689**, L89 (2008).

[9] Marta Volonteri, Kayhan Gültekin, and Massimo Dotti, Gravitational recoil: Effects on massive black hole occupation fraction over cosmic time, Mon. Not. R. Astron. Soc. **404**, 2143 (2010).

[10] A. Sesana, Extreme recoils: Impact on the detection of gravitational waves from massive black hole binaries, Mon. Not. R. Astron. Soc. **382**, L6 (2007).

[11] Pau Amaro-Seoane *et al.*, Laser interferometer apace antenna, arXiv:1702.00786.

[12] J. Aasi *et al.* (LIGO Scientific Collaboration), Advanced LIGO, Classical Quantum Gravity **32**, 074001 (2015).

[13] F. Acernese *et al.* (Virgo Collaboration), Advanced Virgo: A second-generation interferometric gravitational wave detector, Classical Quantum Gravity **32**, 024001 (2015).

[14] S. E. Woosley, Pulsational pair-instability supernovae, Astrophys. J. **836**, 244 (2017).

[15] Pablo Marchant, Mathieu Renzo, Robert Farmer, Kaliroe M. W. Pappas, Ronald E. Taam, Selma de Mink, and Vassiliki Kalogera, Pulsational pair-instability supernovae in very close binaries, Astrophys. J. **882**, 36 (2019).

[16] R. Abbott *et al.* (LIGO Scientific, Virgo Collaborations), GW190521: A Binary Black Hole Merger with a Total Mass of 150 $M_{\odot}$, Phys. Rev. Lett. **125**, 101102 (2020).

[17] R. Abbott *et al.* (LIGO Scientific, Virgo Collaborations), GWTC-2: Compact Binary Coalescences Observed by LIGO and Virgo During the First Half of the Third Observing Run, Phys. Rev. X **11**, 021053 (2021).

[18] R. Abbott *et al.* (LIGO Scientific, VIRGO, KAGRA Collaborations), GWTC-3: Compact binary coalescences observed by LIGO and Virgo during the second part of the third observing run, arXiv:2111.03606.

[19] Davide Gerosa and Maya Fishbach, Hierarchical mergers of stellar-mass black holes and their gravitational-wave signatures, Nat. Astron. **5**, 749 (2021).

[20] Tamara Bogdanovic, M. Coleman Miller, and Laura Blecha, Electromagnetic counterparts to massive black hole mergers, arXiv:2109.03262.

[21] Vijay Varma, Maximiliano Isi, and Sylvia Biscoveanu, Extracting the Gravitational Recoil from Black Hole Merger Signals, Phys. Rev. Lett. **124**, 101104 (2020).

[22] R. Abbott *et al.* (LIGO Scientific, Virgo Collaborations), Properties and astrophysical implications of the 150 $M_{\odot}$ binary black hole merger GW190521, Astrophys. J. **900**, L13 (2020).

[23] Davide Gerosa and Christopher J. Moore, Black Hole Kicks as New Gravitational Wave Observables, Phys. Rev. Lett. **117**, 011101 (2016).

[24] J. Calderón Bustillo, J. A. Clark, P. Laguna, and D. Shoemaker, Tracking Black Hole Kicks from Gravitational Wave Observations, Phys. Rev. Lett. **121**, 191102 (2018).

[25] Carlos O. Lousto and James Healy, Kicking gravitational wave detectors with recoiling black holes, Phys. Rev. D **100**, 104039 (2019).

[26] James Healy, Carlos O. Lousto, Jacob Lange, and Richard O'Shaughnessy, Application of the third RIT binary black hole simulations catalog to parameter estimation of gravitational waves signals from the LIGO-Virgo O1/O2 observational runs, Phys. Rev. D **102**, 124053 (2020).

[27] Parthapratim Mahapatra, Anuradha Gupta, Marc Favata, K. G. Arun, and B. S. Sathyaprakash, Remnant black hole kicks and implications for hierarchical mergers, Astrophys. J. Lett. **918**, L31 (2021).

[28] B. P. Abbott *et al.* (LIGO Scientific, Virgo Collaborations), GWTC-1: A Gravitational-Wave Transient Catalog of Compact Binary Mergers Observed by LIGO and Virgo during the First and Second Observing Runs, Phys. Rev. X **9**, 031040 (2019).

[29] R. Abbott *et al.* (LIGO Scientific, Virgo Collaborations), Population properties of compact objects from the second LIGO-Virgo gravitational-wave transient catalog, Astrophys. J. Lett. **913**, L7 (2021).

[30] Mark Hannam, Charlie Hoy, Jonathan E. Thompson, Stephen Fairhurst, Vivien Raymond, and members of the LIGO (VIRGO Collaboration), Measurement of general-relativistic precession in a black-hole binary, arXiv:2112.11300.

[31] Vijay Varma, Sylvia Biscoveanu, Maximiliano Isi, Will M. Farr, and Salvatore Vitale, Hints of Spin-Orbit Resonances in the Binary Black Hole Population, Phys. Rev. Lett. **128**, 031101 (2022).

[32] Zoheyr Doctor, Ben Farr, and Daniel E. Holz, Black hole leftovers: The remnant population from binary black hole mergers, Astrophys. J. Lett. **914**, L18 (2021).

[33] Tousif Islam, Feroz Shaik, Carl-Johan Haster, Vijay Varma, Scott Field, Jacob Lange, Richard O'Shaughnessy, Rory Smith, and Avi Vajpeyi, Re-analysis of GWTC-3 events with numerical relativity surrogate models (to be published).

[34] R. Abbott *et al.* (LIGO Scientific, Virgo Collaborations), GW190814: Gravitational waves from the coalescence of a 23 solar mass black hole with a 2.6 solar mass compact object, Astrophys. J. Lett. **896**, L44 (2020).

[35] Eric Thrane and Colm Talbot, An introduction to Bayesian inference in gravitational-wave astronomy: Parameter estimation, model selection, and hierarchical models, Pub. Astron. Soc. Aust. **36**, e010 (2019).

[36] Rory J. E. Smith, Gregory Ashton, Avi Vajpeyi, and Colm Talbot, Massively parallel Bayesian inference for transient gravitational-wave astronomy, Mon. Not. R. Astron. Soc. **498**, 4492 (2020).

[37] Joshua S. Speagle, DYNESTY: A dynamic nested sampling package for estimating Bayesian posteriors and evidences, Mon. Not. R. Astron. Soc. **493**, 3132 (2020).

[38] Vijay Varma, Scott E. Field, Mark A. Scheel, Jonathan Blackman, Davide Gerosa, Leo C. Stein, Lawrence E. Kidder, and Harald P. Pfeiffer, Surrogate models for precessing binary black hole simulations with unequal masses, Phys. Rev. Research **1**, 033015 (2019).

[39] V. Varma, D. Gerosa, L. C. Stein, F. Hébert, and H. Zhang, High-Accuracy Mass, Spin, and Recoil Predictions of Generic Black-Hole Merger Remnants, Phys. Rev. Lett. **122**, 011101 (2019).

[40] G. Pratten, C. García-Quirós, M. Colleoni, A. Ramos-Buades, H. Estellés, M. Mateu-Lucena, R. Jaume, M. Haney, D. Keitel, J. E. Thompson, and S. Husa, Computationally efficient models for the dominant and subdominant harmonic modes of precessing binary black holes, Phys. Rev. D **103**, 104056 (2021).

[41] S. Ossokine, A. Buonanno, S. Marsat, R. Cotesta, S. Babak, T. Dietrich, R. Haas, I. Hinder, H. P. Pfeiffer, M. Pürrer, C. J. Woodford, M. Boyle, L. E. Kidder, M. A. Scheel, and B. Szilágyi, Multipolar effective-one-body waveforms for precessing binary black holes: Construction and validation, Phys. Rev. D **102**, 044055 (2020).

[42] Fabian Hofmann, Enrico Barausse, and Luciano Rezzolla, The final spin from binary black holes in quasi-circular orbits, Astrophys. J. **825**, L19 (2016).

[43] Enrico Barausse, Viktoriya Morozova, and Luciano Rezzolla, On the mass radiated by coalescing black-hole binaries, Astrophys. J. **758**, 63 (2012); **786**, 76(E) (2014).

[44] Xisco Jiménez-Forteza, David Keitel, Sascha Husa, Mark Hannam, Sebastian Khan, and Michael Pürrer, Hierarchical data-driven approach to fitting numerical relativity data for nonprecessing binary black holes with an application to final spin and radiated energy, Phys. Rev. D **95**, 064024 (2017).

[45] Carlos O. Lousto, Yosef Zlochower, Massimo Dotti, and Marta Volonteri, Gravitational recoil from accretion-aligned black-hole binaries, Phys. Rev. D **85**, 084015 (2012).

[46] Vijay Varma, Scott E. Field, Mark A. Scheel, Jonathan Blackman, Lawrence E. Kidder, and Harald P. Pfeiffer, Surrogate model of hybridized numerical relativity binary black hole waveforms, Phys. Rev. D **99**, 064045 (2019).

[47] J. Blackman, S. E. Field, M. A. Scheel, C. R. Galley, C. D. Ott, M. Boyle, L. E. Kidder, H. P. Pfeiffer, and B. Szilágyi, Numerical relativity waveform surrogate model for generically precessing binary black hole mergers, Phys. Rev. D **96**, 024058 (2017).

[48] See Supplemental Material at http://link.aps.org/supplemental/10.1103/PhysRevLett.128.191102 for tests of the surrogate models using high spin NR injections, which includes Refs. [49–54].

[49] Michael Boyle *et al.*, The SXS Collaboration catalog of binary black hole simulations, Classical Quantum Gravity **36**, 195006 (2019).

[50] Marissa Walker, Vijay Varma, and Geoffrey Lovelace, Extending numerical relativity surrogate models to near extremal spins (to be published).

[51] Mark A. Scheel, Matthew Giesler, Daniel A. Hemberger, Geoffrey Lovelace, Kevin Kuper, Michael Boyle, B. Szilágyi, and Lawrence E. Kidder, Improved methods for simulating nearly extremal binary black holes, Classical Quantum Gravity **32**, 105009 (2015).

[52] LIGO Scientific Collaboration, Updated Advanced LIGO sensitivity design curve, Technical Report (2018), https://dcc.ligo.org/LIGO-T1800044/public.

[53] SXS Collaboration, The SXS collaboration catalog of gravitational waveforms, http://www.black-holes.org/waveforms.

[54] Katerina Chatziioannou, Geoffrey Lovelace, Michael Boyle, Matthew Giesler, Daniel A. Hemberger, Reza Katebi, Lawrence E. Kidder, Harald P. Pfeiffer, Mark A. Scheel, and Béla Szilágyi, Measuring the properties of nearly extremal black holes with gravitational waves, Phys. Rev. D **98**, 044028 (2018).

[55] I. M. Romero-Shaw *et al.*, Bayesian inference for compact binary coalescences with bilby: Validation and application to the first LIGO–Virgo gravitational-wave transient catalogue, Mon. Not. R. Astron. Soc. **499**, 3295 (2020).

[56] Vijay Varma, Maximiliano Isi, Sylvia Biscoveanu, Will M. Farr, and Salvatore Vitale, Measuring binary black hole orbital-plane spin orientations, Phys. Rev. D **105**, 024045 (2022).

[57] The posteriors for $\chi_1, \chi_2$, and $q$ are expected to be consistent between the two reference points (modulo parameter estimation uncertainty) as these parameters are independent of the reference point.

[58] Fabio Antonini and Frederic A. Rasio, Merging black hole binaries in galactic nuclei: Implications for advanced-LIGO detections, Astrophys. J. **831**, 187 (2016).

[59] G. Monari, B. Famaey, I. Carrillo, T. Piffl, M. Steinmetz, R. F. G. Wyse, F. Anders, C. Chiappini, and K. Janßen, The escape speed curve of the Galaxy obtained from Gaia DR2 implies a heavy Milky Way, Astron. Astrophys. **616**, L9 (2018).

[60] The Kullback–Leibler 300 (KL) divergence [61] from the prior to the posterior in Fig. 2 is 4.3 bits. By contrast, the largest KL divergence for the events considered in Ref. [21] was 0.22 bits.

[61] S. Kullback and R. A. Leibler, On information and sufficiency, Ann. Math. Stat. **22**, 79 (1951).

[62] Sizheng Ma, Matthew Giesler, Vijay Varma, Mark A. Scheel, and Yanbei Chen, Universal features of gravitational waves emitted by superkick binary black hole systems, Phys. Rev. D **104**, 084003 (2021).

[63] R. Abbott *et al.* (LIGO Scientific, VIRGO, KAGRA Collaborations), Tests of general relativity with GWTC-3, arXiv:2112.06861.

[64] vijayvarma392.github.io/GW200129/#kick.

[65] LIGO Scientific Collaboration and Virgo Collaboration, Gravitational Wave Open Science Center, https://www.gw-openscience.org.